Structural Analysis of Historical Constructions, New Delhi 2006
P.B. Lourenço, P. Roca, C. Modena, S. Agrawal (Eds.)

FE Modelling and Material Characterization of Tahir ile Zühre Mescidi, Konya, Turkey

Yasemin D. Aktaş
Middle East Technical University, Archaeometry Graduate Program, Graduate School of Natural and Applied Sciences, Ankara, Turkey

Ahmet Türer
Middle East Technical University, Structural Engineering Lab., Department of Civil Engineering, Ankara, Turkey

Emine N. Caner-Saltık
Middle East Technical University, Restoration Graduate Program, Department of Architecture, Ankara, Turkey

ABSTRACT: The aim of this study was to investigate the structural behaviour of a historic monument in relation with its material characteristics. For this purpose, Tahir ile Zühre Mescidi in Konya, Turkey, a 13th century brick-masonry structure, was chosen as the case study. The basic physical and mechanical material characteristics that need to be defined in the FE modelling were determined through a series of laboratory material tests. A 3D-FE model of the superstructure was constructed using commercially available structural analysis software SAP2000. Smeared joint method was used to model mortar-brick interfaces. The model was first analyzed under dead load, wind load, and snow load. The behavior of the 8 centuries old structure under normal service conditions was simulated and performance approved by the analysis results. Secondly, a concrete coating layer was simulated over the dome and the temperature induced forces and strains at the interface were studied. The crack formation and delamination that a concrete coating might cause was simulated.

1 INTRODUCTION

Masonry has been (and still is) one of the most popular construction techniques due to its advantageous characteristics including economy, durability, heat insulation characteristics and sufficient compressive strength of the materials. However, a limitation factor of masonry is its low tensile strength, which could cause serious problems at the existence of considerable lateral forces (such as earthquakes), significant differential settlements, and/or out-of-plane bending (Lu et al. 2005).

Studies on analytical and material aspects of ancient masonry monuments are recently attracting larger attention. The interaction between the analytical studies and material properties becomes more important, and powerful analytical models can now be generated using advanced computer programs and structural identification especially through material, static, and dynamic testing.

The aim of this study was to investigate the effect of material characteristics, both physically and mechanically, on the structural behaviour of a historic structure. In addition, how the structural behaviour would be affected by wrong repairs such as concrete coating. For this purpose, the domed superstructure of Tahir ile Zühre Mescidi in Konya, Turkey, which is a 13th century brick-masonry small mosque structure, namely 'masjid' was chosen as case study. The superstructure is composed of a dome and squinches, providing the transition from circular dome to a square plan. At three sides of the dome, there are window openings between the squinches while one side is totally closed. The structure reflects the characteristics of Anatolian Seljuk period both in terms of construction technology and architecture, at which brick was used for structural as well as decoration purposes. Although the structure is not in a good conservation state, it does not have any structural defects such as structural cracks or important material deterioration.

2 EXPERIMENTAL STUDIES ON DETERMINING MATERIAL CHARACTERISTICS

For a structural analysis to be able to reflect the structural behaviour of the monument in a verisimilar manner, certain aspects of modelling, such as geometry, element type selection, meshing, boundary conditions, compatibility of different types of elements, and material properties should be defined correctly. In the case of a historic structure, determination of original material properties by an extensive material investigation gains further importance because the material properties often have composite nature, such as brick and mortar. Furthermore, the material properties might be nonhomogeneous throughout the building. Long term behavior and aging of the monument also affects the material characteristics. All these factors related with the material properties may render the assessment of structural condition and behavior misleading if not supported with correct material data (Zucchini 2004). The structural analysis through numerical approaches, therefore, should be supported with laboratory analyses of materials, as well as in situ investigation, whenever possible.

For these reasons, the study was started initially with the investigation of the materials composing masonry, i.e. the original brick and mortar, through a series of laboratory analyses. These laboratory studies included the determination of the physical and mechanical properties of materials, i.e. bulk density and modulus of elasticity. For the determination of modulus of elasticity, ultrasonic velocity method, which is a non-destructive technique, was used. Then, a correlation was developed between the modulus of elasticity and uniaxial compressive strength of the materials, using the experimental data obtained previously for a large set of mortar samples belonging to the aforementioned period. For material tests, a total of 24 brick and 2 mortar samples taken from the brick masonry upper structure were used in this study.

2.1 Bulk density test

For the determination of bulk density, the samples were dried in the oven at 35ºC to constant weight (until the difference between two successive weighing at an interval of 24 hours, is not more than 0.1% of the sample weight (TEUTONICO 1988). These weight measurements were recorded as the dry weights of the samples (m_{dry}). The saturation of samples in distilled water was carried out in a vacuum at about 0.132 atm pressure. The weights of the water-saturated samples were recorded as saturated weights (m_{sat}). The weights of saturated samples were measured also in water and recorded as Archimedes weight (m_{arch}). They were used in the calculation of bulk density of the samples as follows (RILEM 1980):

$$D(g/cm^3) = m_{dry}/(m_{sat} - m_{arch}) \quad (1)$$

where, m_{sat}: saturated weight (g), m_{dry}: dry weight (g), and m_{arch}: the weight of the sample in water (g). The results of bulk density test carried out for 20 brick and 2 mortar samples are as follows:

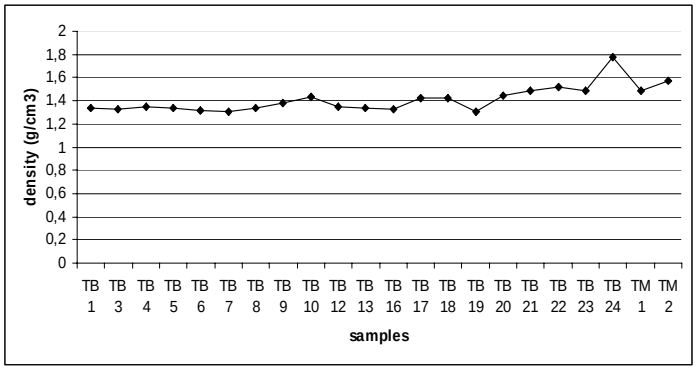

Figure 1 : Variation in bulk density values (g/cm³) of the samples

2.2 Modulus of elasticity test

The modulus of elasticity was determined by ultrasonic pulse velocity measurements (ASTM D 2845-90, RILEM 1980). A pulse generating test equipment, PUNDIT*plus*, with its 220 kHz

transmitter and receiver probes, was used. This method was based on the measurement of the time required for the ultrasonic waves to travel the minimum cross section of the test specimen. The velocity of the waves was calculated by using Eq. (2) (RILEM 1980, ASTM D 2845-90).

$$V = l/t \tag{2}$$

where, V = ultrasonic velocity (mm/s), l = the distance traveled by the wave (cross section of test specimen) (mm), and t = travel time (s).

The modulus of elasticity was then obtained through the bulk density of the specimen and ultrasonic velocity using the Eq. (3) (RILEM, 1980)

$$E_{\text{mod}} = D*V^2(1+\nu_{dyn})(1-2\nu_{dyn})/(1-\nu_{dyn}) \tag{3}$$

where, E_{mod} = modulus of elasticity (Pa), D = bulk density of the specimen (kg/m^3), V = wave velocity (m/s) and ν_{dyn} = Poisson's ratio (0.20 was used for the calculations here, since it is a commonly accepted value in literature for historic masonry material, such as Carpinteri et al. (2005) Ramos et al. (2004). The results are given in Fig. 2 for 18 brick and 2 mortar samples.

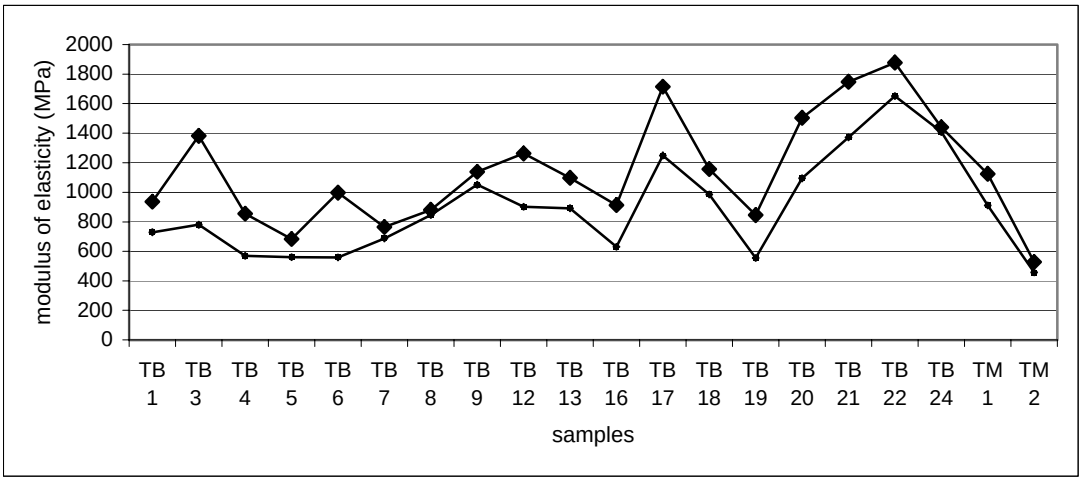

Figure 2 : Variation in modulus of elasticity (Young's Modulus) values (MPa) of the samples in dry and wet state (dry and wet states are shown with diamond and square marks, respectively)

2.3 Uniaxial compressive strength test

For the aim of determining uniaxial compressive strengths, a data set obtained in a previous study of uniaxial compressive strength versus modulus of elasticity was used. In this previous study, both uniaxial compressive strengths and moduli of elasticity of a series of mortar samples taken from more than 20 Seljuk period monuments were determined experimentally, by point load testing and ultrasonic velocity method, respectively. A correlation between modulus of elasticity and uniaxial compressive strengths was developed using the mentioned data set by us. A second order polynomial was curve fitted to the data and Eq. (4) was obtained.

$$UCS = -10^{-6}(E_{\text{mod}})^2 + 0.0056(E_{\text{mod}}) - 0.2953 \tag{4}$$

Therefore, the UCS values were estimated for 18 brick and 2 mortar samples as shown in Fig. 3.

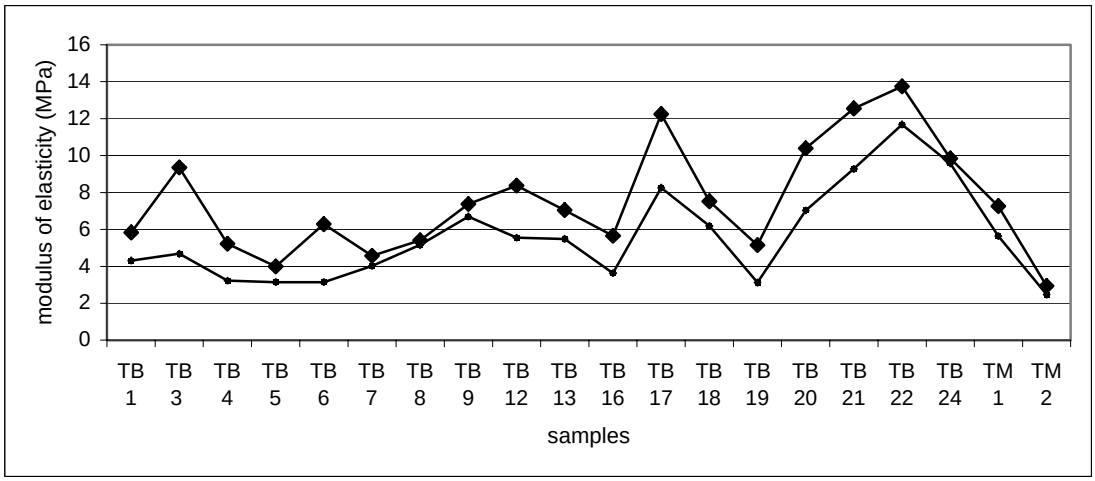

Figure 3 : Variation in uniaxial compressive strength values (MPa) of the samples in dry and wet state (dry and wet states are shown with diamond and square marks, respectively)

3 FINITE ELEMENT MODELING STUDIES

3.1 Introduction

For the structural analysis of the super structure of the masjid, which is composed of a dome and squinches, a finite element (FE) model was constructed, in accordance with its actual geometry. The material properties obtained from the lab tests were incorporated into the structural analysis using SAP2000.

Masonry requires a special method of analysis due to its non-homogeneity, anisotropy, asymmetry in tension and compression, and non-linearity, which are caused by the presence of mortar joints in both directions as well as material properties (Lu *et al.*, 2005).

The modeling of mortar interface between brick blocks can be achieved by means of three different approaches: a) discontinuous element modeling, b) discrete element modeling, and c) smeared joint modeling (macromodelling) (Lu *et al.*, 2005, Zucchini, 2004). In this study, the last approach, macromodelling was used, which is efficient, simple, and sufficiently accurate (Lu *et al.*, 2005). According to this approach, a homogenization process was carried out such that the composite material was assumed to behave as a continuum whose properties are an average of those of bricks and mortar.

For the first part of the study three different loads were assigned: (1) self-load, (2) wind load, and (3) snow load. Then, the same model was analyzed for the case of a concrete coating of 10 cm in thickness. For wind and snow loads, Turkish Standards (TS 498) was considered. All models were analyzed linearly.

The uniaxial compressive strength values of brick and mortar determined by the laboratory tests were extrapolated into an integrated value for masonry according to EUROCODE 6.

$$f_k = K * f_b^{0.65} * f_m^{0.25} (N/mm^2) \tag{5}$$

where, f_k = strength of masonry, f_b = strength of brick (12 MPa), f_m = strength of mortar (4.5 MPa), and K = a constant of 0.60. Using Eq. (5), the uniaxial compressive strength of masonry was found as 4.4 MPa. In this study, the tensile strength of masonry was taken as 0.4 MPa, which is about 1/10 of the compressive strength.

For defining modulus of elasticity for the composite material, compatibility of deformations principle was applied to Hooke's law as shown in Eq. (6).

$$\frac{t_{brick} + t_{mortar}}{E_e} = \frac{t_{brick}}{E_{brick}} + \frac{t_{mortar}}{E_{mortar}} \tag{6}$$

At Tahir ile Zühre Mescidi, t_{brick} and t_{mortar} were taken as 9 cm and 3 cm, respectively. E_{brick} and E_{mortar} were taken as 1100 MPa and 800 MPa, respectively for the smeared average values.

By using the Eq. (6), E_e was approximately found as 1005 MPa. The wall thickness of the dome is about 65cm which is formed by layers of bricks placed side by side. Possible cover concrete is considered to be 10cm in thickness.

As mentioned before, the analyses were carried out only at the superstructure of the masjid, including the dome and squinches. The restraint conditions were assumed to be fixed ends since the shape of the squinches, wall thickness, weight of the superstructure, and substructure rigidity supports this assumption. Any divergence from the fixed end support condition is assumed to be insignificant. The unsymmetric geometry caused by the window openings is correctly modelled. As seen in Fig. 4, at three sides of the dome, between the squinches, there are window openings, while one side is totally closed.

3.2 FE model #1 (using shell members) analysed under a combination of dead load, snow load, and wind load

For the purpose of analyzing the structure under a combination of dead load (SELF), snow load (SL) and wind load (WLX), a shell model was constructed with using 2448 shell elements.

Because an existing monument was analysed, normal service conditions were investigated. Therefore, design factors and safety coefficients were not used. In the load combinations, different loading effects were linearly added to each other. To define wind and snow loads, TS 498 was utilized. The reaction forces are listed in Table 1, which indicates that the maximum force is created by the self weight. When lateral forces are considered, wind load is insignificant, while earthquake load is expected to be the dominant lateral force exerted on the structure.

Table 1: Base reactions under dead load, snow load and wind load

OutputCase	GlobalFX	GlobalFY	GlobalFZ
	N	N	N
SELF	2,013E-07	2,499E-07	721741,62
SL	1,003E-08	1,24E-08	21014,68
WLX	-10957,31	-1,646E-09	-3,623E-08

3.3 FE model #2 (using shell members with rigid links) 10 cm concrete coating over masonry dome analysed under a combination of dead load and uniform temperature load of 40ºC

For simulating the case that the superstructure is covered with a concrete coating of 10 cm in thickness, the pre-constructed shell model with 2448 shell elements is connected to another shell model covering the original dome and representing a concrete coating with 2448 areas. The connection between two dome layers is provided by frame element links. Sensitivity analysis was performed to understand the level of fixity between two dome layers imposed by the links.

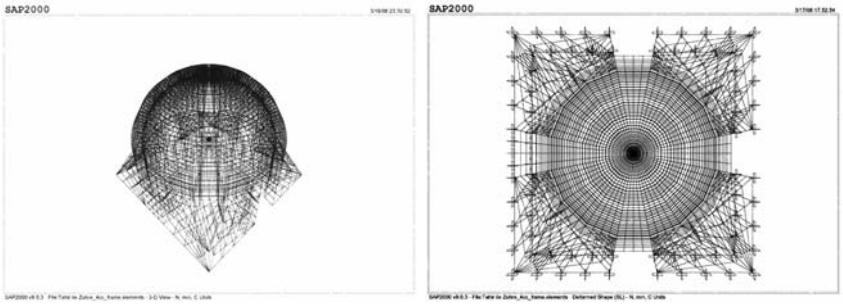

Figure 4 : A 3D view and bottom view of the superstructure composed of two layers connected with rigid links to analyse under temperature load

In this part of the study, possibility of crack formation on the concrete coating, covering masonry dome, was investigated. Furthermore, separation (delamination) of the coating and masonry dome is investigated. The model was analysed under a combination of dead load and a uniformly distributed temperature load of 40ºC. Sensitivity analysis of the rigid link stiffness revealed the flexible and rigid regions of the link as a function of moment of inertia (I). The moment values developing on the rigid links are close to zero for low I values ($I<1e6\ mm^4$),

while moments increase and approach to a constant value for high I values (I<1e9 mm^4). The rigid link frame members become semi-rigid for 1e6 mm^4 < I < 1e9 mm^4.

The simulation was started by defining rigid frames between dome and cover layers to see the stress concentration locations where delamination will start. Tensile stresses developing at the cover concrete and masonry dome are investigated for crack formation.

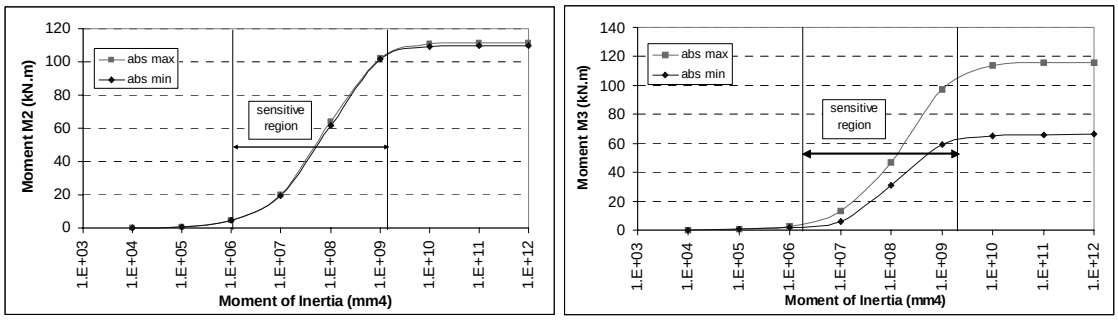

Figure 5 : Graphs of minimum and maximum M2 and M3 values (i.e. bending moments in the 1-3 and 1-2 planes with square and diamond markers, respectively) as a function of moment of inertia (under dead load and 40ºC uniform temperature load)

The coefficients of thermal expansion of concrete and masonry material were assigned as $10x10^{-6}$ $ºC^{-1}$ and $7x10^{-6}$ $ºC^{-1}$, respectively. Therefore, under a positive temperature change the concrete coat would try to expand more in comparison to the masonry dome generating tensile stresses in the dome. During winter, the concrete coating is expected to try shrinking causing tension cracks in the concrete coating. As it can be seen from Fig. 6, the tensile stresses developing in the concrete coating exceed the tensile capacity of concrete for a temperature difference of 40 C^o ($I = 10^9$ mm^4).

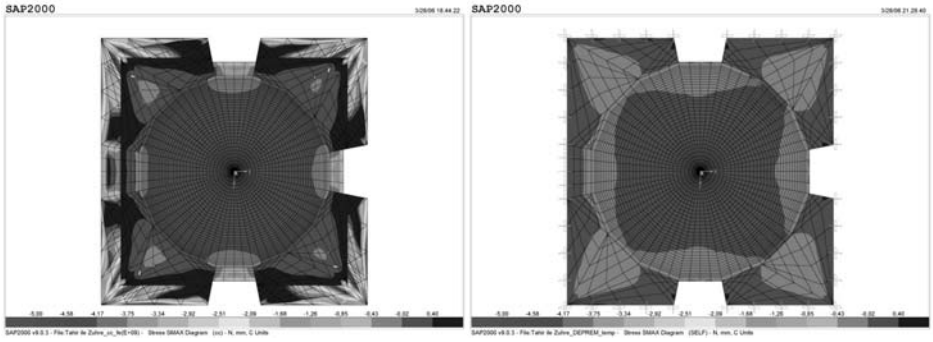

Figure 6 : Bottom view of resulting SMAX diagrams of the superstructure with and without concrete cover, respectively (under dead load and 40ºC uniform temperature load; $I=10^9$ mm^4)

The bending moment diagram obtained for the link members between dome and concrete cover is an indication of shear developing between the two layers (Fig. 7). Shear forces between the two layers is maximum at the squinches region as an indication of the most probable location to start the delamination process. The maximum stresses developing in the cover concrete also shows the maximum tension stress zones in Fig. 8. Tensile stresses in the order of 3 MPa cannot be tolerated by the cover concrete and cracking-delamination is inevitable. Simulation of delamination by reducing the I value to semi-rigid zone ($I=10^8$ mm^4) in the critical sections results in small reduction in the stress levels, critical link members and the stress distributions remain the same; therefore, excessive damage is required to change the stress distribution.

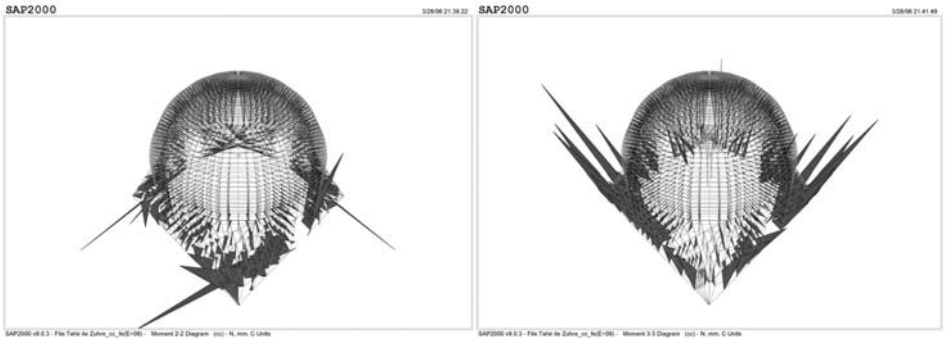

Figure 7 : Resulting 3D moment diagrams in 1-3 and 1-2 directions, respectively (under dead load and 40ºC uniform temperature load; I=10^9 mm^4)

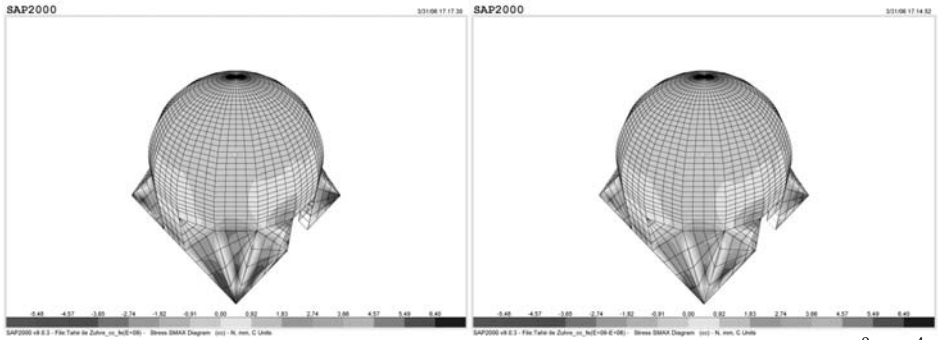

Figure 8 : 3D Smax diagrams for the case that the moment of inertia of the system is 10^9 mm^4 and that of critical frames were reduced to 10^8 mm^4 respectively

The maximum (tensile) stress distribution Smax, similar to Fig. 8, is obtained from the bottom view in Fig. 9. The maximum tensile stresses slightly decrease in the case when the moment of inertia (I) values of the critical frames were decreased from 10^9 mm^4 to 10^8 mm^4. Nevertheless, the maximum tensile stresses developing in the masonry dome and concrete cover due to a uniform temperature loading of 40 C^o are beyond the accepted tensile capacity limits of the masonry dome and concrete cover materials; 0.4 MPa and 2 MPa, respectively. Even The maximum tensile stress concentrations are obtained at the window opening corners for the concrete cover and at the top of window openings and base level for the masonry dome. the weight of the concrete dome is found to be inadequate and tensile stresses exceed 0.4 MPa limit.

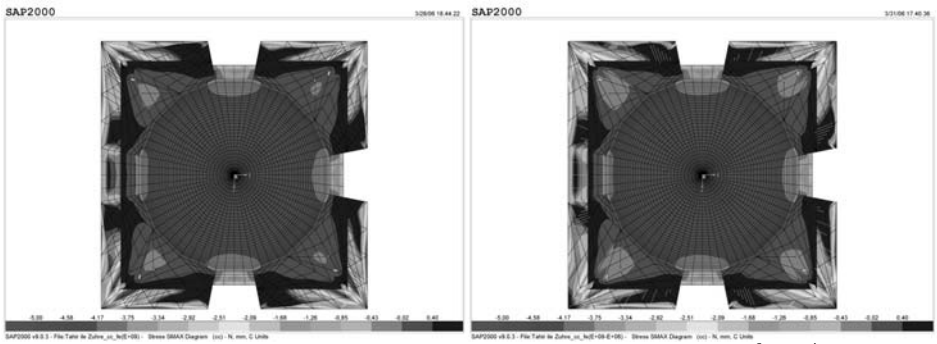

Figure 9 : Bottom views of Smax diagrams when moment of inertia (I) is 10^9 mm^4 and I of critical frames reduced to 10^8 mm^4, respectively

3.4 FE model #3 (using shell members with rigid links) 10 cm concrete coating over masonry dome analysed under a combination of dead load and randomly distributed temperature load of 25ºC

At this last stage of the study, to render the results more observable in real life, the same model composed of 2448 shell elements representing masonry superstructure linked, by rigid links to

another 2448 shell elements representing cement coating of 10 cm in thickness, was analyzed under a partially acting temperature load of 25 °C (Fig. 10).

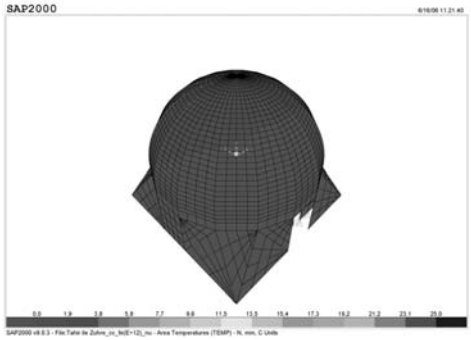

Figure 10 : Applied temperature load of 25ºC. Dark blue indicates the part warmer.

Also in this case, a sensitivity analysis was carried out to see where delamination process begins. As seen Fig. 11, the sensitive region in this case is found similar to the previous study and between $I=10^6$ mm^4 and $I=10^9$ mm^4.

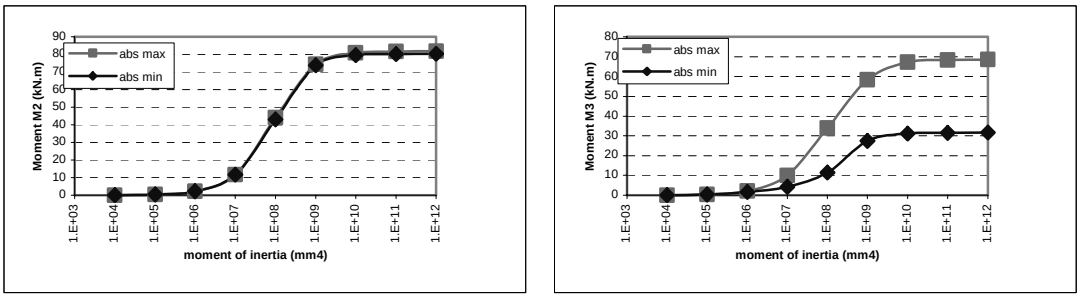

Figure 11 : Graphs of minimum and maximum M2 and M3 values (i.e. bending moments in the 1-3 and 1-2 planes with square and diamond markers, respectively) as a function of moment of inertia.

For the moment of inertia value equal to 10^9 mm^4, the resulting tensile stresses at the inner face of the masonry dome get close to 1 MPa, at the very bottom of the squinches at the side which temperature load was applied (positive y direction). At the outer face, on the other hand, at the limits of the temperature application area, the resulting tensile stresses reaches to even 3 MPa, which is commonly beyond the tensile cracking capacity of concrete (Fig. 12 and 13).

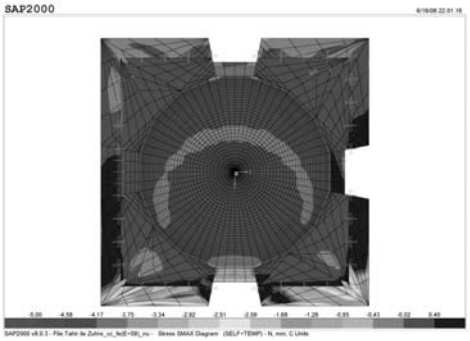

Figure 12 : Bottom view of resulting SMAX diagrams of the superstructure with concrete cover (under dead load and 25ºC randomly distributed temperature load)

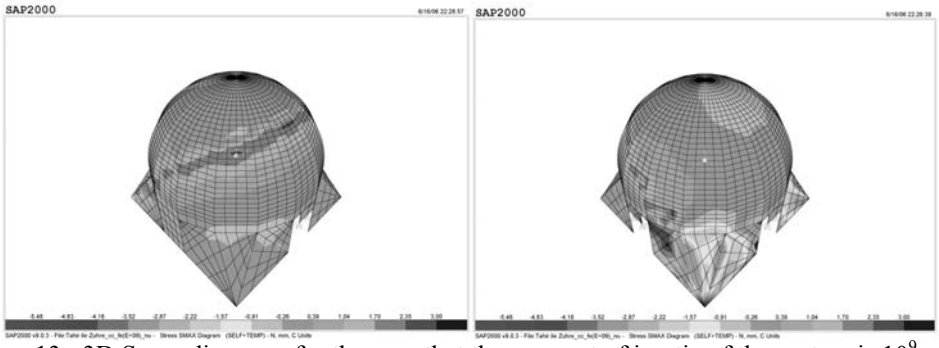

Figure 13 : 3D Smax diagrams for the case that the moment of inertia of the system is 10^9 mm^4

Figure 14 : Resulting 3D moment diagrams in 1-3 and 1-2 directions, respectively (under dead load and 25ºC randomly distributed temperature load; I=10^9 mm^4)

The critically loaded frames were also determined: They appeared at the very bottom line of the superstructure and, in the direction of the application of temperature load (positive y), also at the squinces. The moments of inertia of these frames were reduced down to 10^8 mm^4. The resulting stress distribution is shown in Fig. 15 for bottom view and both sides of the superstructure under investigation which is similar to the case obtained in Fig. 13.

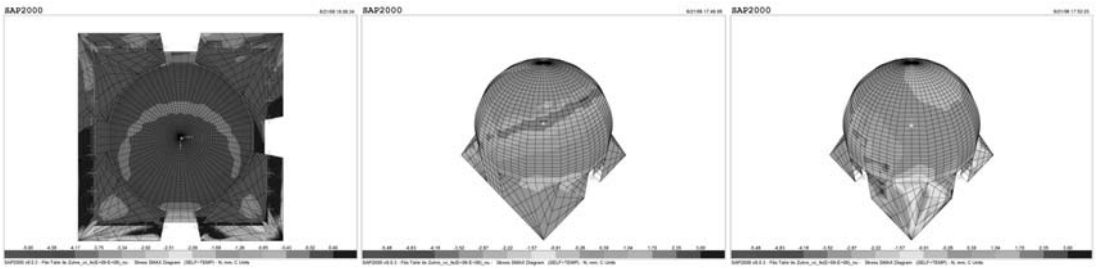

Figure 15 : Bottom and 3D views of resulting SMAX diagrams of the superstructure with concrete cover for the case that the moments of inertia of critical frames were reduced to 10^8 mm^4 (under dead load and 25ºC randomly distributed temperature load)

As seen at the stress diagram, the maximum tensile stress develops at the sides of window opening in the direction of the application of temperature load for masonry material. For concrete cover, on the other hand, the maximum tensile stress formation occurs at the limits of the area where temperature load was applied. Therefore, concrete coating is expected to crack at the temperature gradient regions and squinces.

4 CONCLUSIONS

In this study, material samples taken from Tahir ile Zühre Mescidi in Konya, Turkey were analyzed in laboratory. The material analyses of the 13th century brick-masonry structure revealed that the original construction materials have very low density, in the order of 1.4 g/cm^3.

Modulus of elasticity values obtained by ultrasonic velocity measurements were not constant and scattered between 600 MPa and 1800 MPa. The correlation developed between modulus of elasticity and uniaxial compressive strength was based on load tests which were carried out only on mortar samples by other researchers (Tuncoku, 2001). Although the uniaxial compressive strength values obtained that way appear to be low in comparison with the values given in the literature for historic structures, the crushing will initiate at mortar level and mortar strength is a reasonable limit level for damage criteria. Furthermore, the compressive strength of masonry building materials and related surface areas are generally too large for damage; therefore, the damage is commonly initiated by principal tension stresses developing at the mortar level.

The second part of the study including FE modelling and structural analyses showed that the structure is safe under normal service conditions. The stress values developing under the combination of dead load, snow load, and wind load are much lower than the capacity of the material. On the other hand, additional modelling studies that consider a possible 10cm cover concrete and 40 C^o temperature loading combined with dead load showed development of much higher tensile stresses due to the differences between thermal expansion coefficients of masonry and concrete materials. To simulate an eventual detachment between the layers, frame elements were defined to connect masonry dome and concrete cover. Sensitivity analysis results indicated the ranges of moment of inertia (I) values that cause rigid and flexible connection conditions between the dome and cover. Examining the forces on the frame elements and stresses on the shell elements, critical regions that have high stress concentrations were observed. Detachment zones were formed at the base of the dome and at the openings of squinches due to high tensile stresses. Therefore, it is concluded that crack development is expected at the bottom of the dome and at the corner of squinches, under defined circumstances. The last structural analysis, on the other hand, showed that detachment is expected to occur at the bottom elevation, at the squinches in the direction of temperature application, and at the temperature gradient locations on concrete cover. This study clearly showed that the damage to the dome and cover itself is inevitable in the case of such an inappropriate restoration work using incompatible materials such as concrete. According to the results of the analysis, it is understood that this kind of a restorative intervention actually harms the original structure; therefore, its application should be avoided.

As a future study, researchers would like to expand the sampling number by developing a larger sample set for a series of Anatolian Seljuk structures, so that a generalization of the construction technology and material properties of the period can be obtained. Structural analyses would be extended to include earthquake loads using response spectrum and time history analyses.

REFERENCES

ASTM D2845-90. 1998. Standard Test Method For Laboratory Determination of Pulse Velocities and Ultrasonic Elastic Constants of Rock. ASTM International

Carpinteri, A., Invernizzi, S., Lacidogna, G. 2005. In Situ Damage Assessment and Nonlinear Modelling of a Historical Masonry Tower. *Engineering Structures* 27, p. 387-395

LU, M. et al. 2005. Application of the Arc-Length Method for the Stability Analysis of Solid Unreinforced Masonry Walls Under Lateral Loads. *Engineering Structures* 27, p. 909-919

Ramos, L.F., Lourenço, P.B. 2004. Modelling and Vulnerability of historical City Centers in Seismic Areas : a Case Study in Lisbon. *Engineering Structures* 26, p. 1295-1310

RILEM; Tentative Recommendations, Comission-25-PEM, Recommended Tests to Measure the Deteriorated Stone and to Assess the Effectiveness of Treatment Methods. *Materiaux and Construction* 13; 1980; 173-253

SAP 2000 – Advanced 9.0.3; Computers and Structures Inc.

Teutonico, J.M. 1988. *A laboratory Manual for Architectural Conservators*. Roma: ICCROM

Tuncoku, S.S. 2001. *Characterization of Masonry Mortars Used in Some Anatolian Seljuk Monuments in Konya, Beysehir and Aksehir*. Unpublished Ph.D Thesis, Restoration Program. Ankara: METU

Zucchini, A., Lourenço, P.B. 2004. The Coupled Homogenization-Damage Model for Masonry Cracking. *Computers and Structures* 82, p. 917-929